

Seismic Performance Evaluation of a Structure Retrofitted Using Steel Slit Dampers with Shape Memory Alloy Bars

Asad Naeem¹, Mohamed Nour Eldin¹, Jinkoo Kim^{1,*}, and Joowoo Kim²

¹Department of Civil and Architectural Engineering, Sungkyunkwan University, Suwon, Korea

²Department of Architectural Engineering, Semyung University, Jecheon, Chungbuk, Korea

Abstract

In this paper, a hybrid slit- shape memory alloy (SMA) energy dissipation device is devised by attaching a SMA bar to each face of a steel slit plate. An analysis model of a SMA bar with super elastic capability is developed using various link elements, and the accuracy of the analysis model is verified by comparing with finite element analysis results. The seismic performance of the hybrid slit damper is verified by incorporating them in seven-story steel structure. The nonlinear dynamic analysis results of the model structure subjected to seven earthquake ground motions show that the addition of SMA bars in slit damper results in significant reduction both in the maximum and the residual deformation compared to those of the structure installed with typical steel slit dampers.

Keywords: shape memory alloy, seismic engineering, slit dampers, self-centering

1. Introduction

Shape memory alloys are state of the art material that have the capability to sustain large deformations, and can also retrieve their original shape by inducing thermal energy. This phenomena is known as the superelastic effect (Fremond, 1996). The multidisciplinary potentials of SMA have attracted the interest of many researchers in field of structural engineering to develop earthquake resistant structures with high performance or smart dampers, beam-column connections, innovative bracing systems and re-centering restraining devices (DesRoches and Smith, 2004). Conventional steel slit dampers which are currently used in earthquake resistant structures are efficient in providing energy dissipation capability, but due to their unrecoverable inelastic deformation permanent residual story drift may remain after an earthquake. Previous studies show that the cost of retrofitting and restoring the structure to original position after an earthquake is so high, it would be more economical to rebuild the building rather than repairing it when the residual inter-story drift ratio is more than 0.5% (McCormick *et al.*, 2008).

There are studies for developing smart energy dissipation devices which have the capability of self-centering after being excited by an earthquake. Clark *et al.* (1995) presented a SMA-based damper, which consists of two groups of parallel pre-tensioned SMA wires. Dolce *et al.* (2000) improved this damper by adding another group of SMA wires functioning as re-centering group. Lin *et al.* (2003) conducted tests on mechanical properties of NiTi wires and developed a simulation model of the self-centering damper. Ocel *et al.* (2004) presented a new steel beam-column connection using shape memory alloys. Ma and Cho (2008) presented a re-centering SMA damper which consists of two groups of SMA wires and two springs, functioning as energy dissipating and re-centering groups, respectively, and the numerical simulation results showed that the SMA damper could reduce the residual deformation of the structure effectively. SMA was also applied to, seismic isolators (Andrawes and DesRoches, 2005), cross-bracing cables (McCormick *et al.*, 2007), FRP composite reinforcements (Wierschem and Andrawes, 2010), buckling restrained braces (Miller *et al.*, 2012), bridge cables (Torra *et al.*, 2013), passive control devices (Jalaeefar and Asgarian, 2014), and retrofit of structures (Ingalkar and Rameshwar, 2014). These studies show that utilizing SMA can improve the seismic performance of structures by providing re-centering capability. However the high cost of SMA materials makes it unfeasible for practical application. Moreover, the finite element softwares generally used for modeling SMA generally requires huge computational time.

Received August 27, 2016; accepted June 19, 2017;
published online December 31, 2017
© KSSC and Springer 2017

*Corresponding author
Tel: +82-31-290-7563, Fax: +82-31-290-7570
E-mail: jkim12@skku.edu

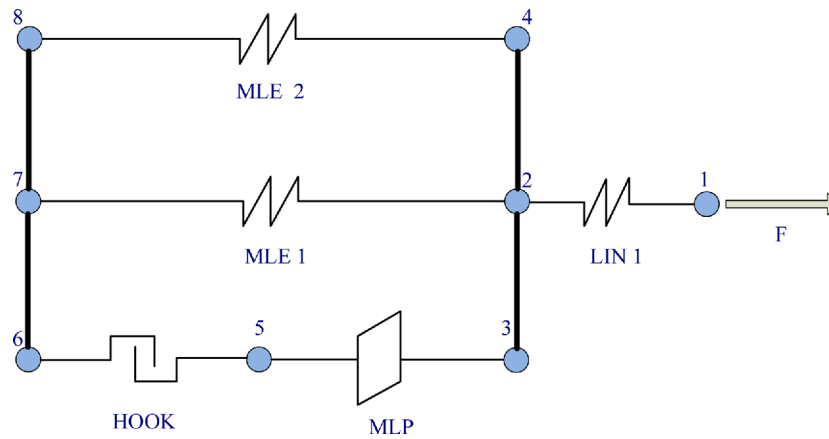


Figure 1. Combination of link elements for modeling of SMA.

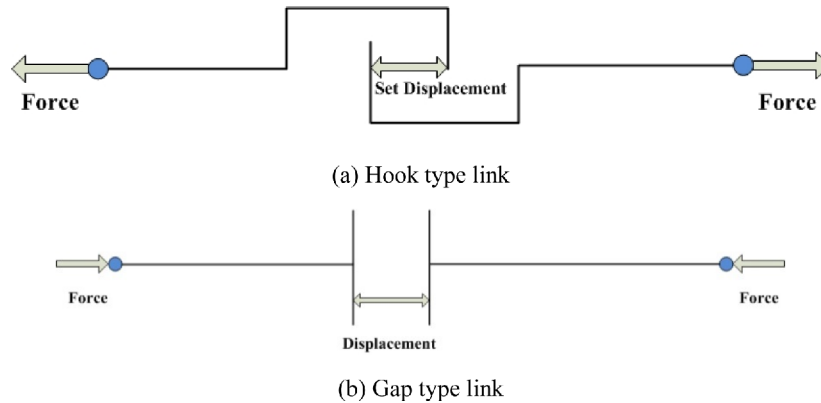


Figure 2. Hook and gap links.

In this work, a hybrid damper consisting of steel slit plate and shape memory alloy (SMA) bars is designed and an analysis model for the damper is developed. The super-elastic characteristics of SMA are modeled in SAP2000 using various link elements and the accuracy of the analysis model is verified by comparing with finite element analysis results. The re-centering performance of the hybrid slit damper is validated by incorporating them in seven-story steel structure and performing non-linear dynamic time history analysis.

2. Characteristics of Shape Memory Alloy

Shape memory alloys (SMAs) display characteristics such as shape memory effect, super-elastic effect, high corrosion resistance, excellent fatigue properties and high damping. SMAs have two main crystalline structures, austenite and martensite states. The transition from one phase to the other can occur by inducing temperature or stress. Martensite state is stable at low temperatures and high stresses while austenite state (parent state) is stable at high temperatures and low stresses. The key characteristic of SMAs is a result of reversible phase transformations between the martensite and austenite phases. Below the martensite finish temperature, M_f , the material has the

shape memory effect and the strain can be recovered by heating the specimen, whereas at a temperature above the austenite finish, A_f , a phenomenon known as the super-elastic effect with a flag shape hysteresis loop occurs (DesRoches *et al.*, 2004). When a sufficiently high stress is applied to the material in the austenite phase, the SMA transforms into the detwinned martensite. When the load is released, a reverse transformation to the austenite state takes place, which results in complete shape recovery and a substantial hysteretic loop. When the stress is released, the martensite transforms back into austenite and the specimen returns to its original shape. This super-elastic effect is utilized in this study to provide a self-centering force to a steel slit damper. It has been shown that the austenitic phase SMAs subjected to a range of up to 8% strain are capable of fully recovering their original shape (DesRoches *et al.*, 2004).

4. Multi-link Modeling for Shape Memory Alloy

In this paper different types of link elements are used to model the super-elastic behavior of SMA bar in the SAP 2000 analysis software. To model the behavior under tensile loads, a hook link is connected in series with a

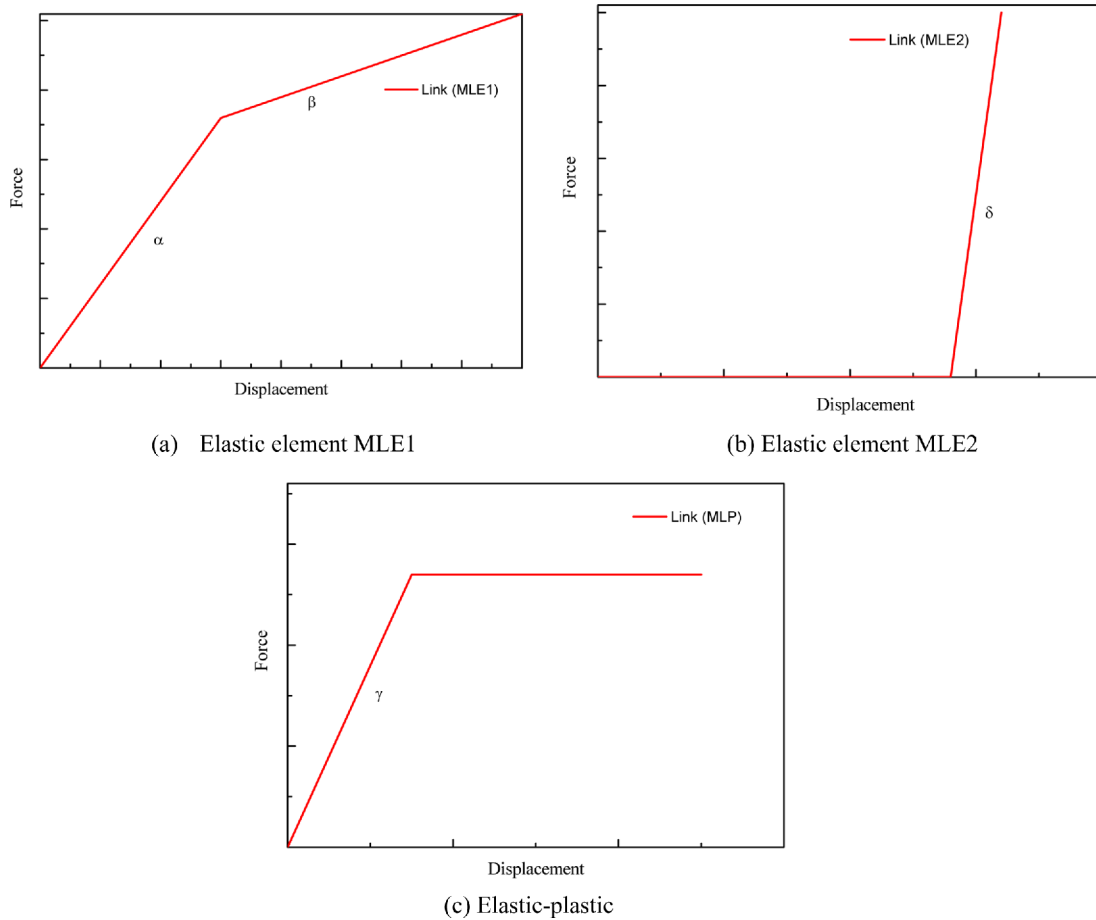


Figure 3. Multi-linear elements for modeling of SMA.

multi linear plastic (MLP) link. They are connected in parallel with two multi linear elastic (MLE1 and MLE2) links. These links are connected in series with a linear (LIN1) link as shown in Fig. 1. The hook link allows certain displacement in one direction; once the set value of displacement is achieved by the force freely, the link ceases to continue displacement in the respective direction (Fig. 2(a)). For compression a gap link is used instead of a hook link, which has opposite function to the hook; it allows compression to certain value, after which it ceases to move (Fig. 2(b)). The linear link behaves like a spring which has stiffness and damping, thus this link element is used to collect the information at one node only without altering the overall effect of other link. Multi-linear elastic links (MLE1 and MLE2) are the combination of two or more linear links, like a spring that permits the change in the stiffness as shown in Fig. 3. In the proposed configuration two multi-linear elastic elements are used (MLE1 and MLE2). The MLE1 link consists of elastic element which has the initial slope of α , and the slope is reduced to β at a certain displacement. The MLE2 link has initial slope of zero for the first interval while it is increased to γ for the next interval. Multi linear plastic link provides the feature of an elastic behavior initially,

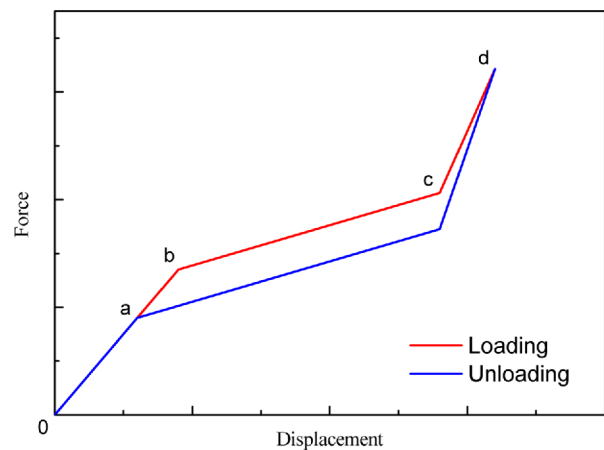


Figure 4. Force-displacement relationship of SMA modeled by link elements.

but at reaching a yield force the link moves into perfectly plastic phase. Figure 4 shows the force-displacement curve of SMA. When tensile force is applied on node 1, the links MLE1, MLE2, Hook, and MLP begin to work. As the hook and the MLP links are in series, the hook allows the device to have displacement of a , during which MPL

Table 1. Properties of shape memory alloys model

SMA Bar	Elastic modulus (MPa)	Diameter (mm)	Length (mm)	σ^{AS} (MPa)	σ^{SA} (MPa)
1	70000	10	100	300	100
2	70000	10	100	500	100

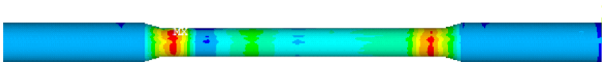


Figure 5. FE model of the SMA bar.

does not work. Since MLE2 has a slope of zero up to point *c*, during this displacement only MLE 1 and Hook links are operational. At point *a*, the hook link has reached the maximum set displacement. In the range between points *a* and *b*, MPL comes in to effect with an elastic gradient. When the model reaches the displacement of *b*, the MLP link becomes plastic. At this stage, only MLE1 works with elastic behavior. Finally when the offset is *c*, MLE2 starts operating simultaneously with MLE1. Similar force-displacement curves can be obtained for compression when buckling is assumed to be prevented using the Gap link instead of the Hook link used in tension.

To validate the accuracy of the proposed model, two SMA bars with different yield stress are analyzed by using the link elements, and the results are compared with those obtained by finite element (FE) analysis using the finite element analysis code ANSYS (2012) which can take into account both geometric and material nonlinearities of SMA. Table 1 shows the dimensions and material properties of the SMA bars used in the analysis, where σ^{AS} and σ^{SA} represent austenite and martensite stresses, respectively. Figure 5 shows the SMA bar modeled with 8-node linear brick finite elements. To check whether the

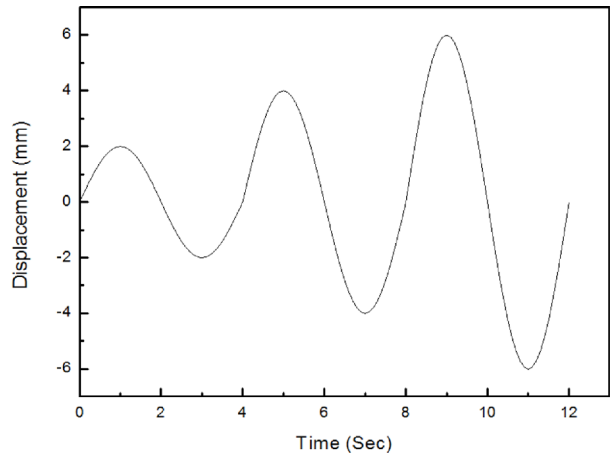


Figure 6. Displacement-controlled cyclic loading.

proposed model works well in compression, the buckling of the bars under compression is prevented in the analysis. Nonlinear analysis is performed on the SMA bars for the displacement-controlled cyclic loading with increasing amplitude shown in Fig. 6. The load is applied in the axial direction of the SMA bars and the stress-strain relationship is computed by direct integration using the Newmark method. Figures 7 and 8 compare the hysteretic curves with superelastic behaviors of the SMA bar specimens 1 and 2, respectively, obtained from the proposed model and the FE analysis. In these curves, all the SMA specimens behave in a similar pattern and show a unique behavior characterized by a flag-shape hysteresis loop under cyclic loading. The results of the proposed model are in good agreement with the finite element analysis results. The hysteresis curves obtained from both the FE analysis and the proposed model show similarities in terms of initial stiffness, yield force, post yielding envelope, unloading stiffness, reloading stiffness, ultimate force, restoring force and stable energy dissipation. Both

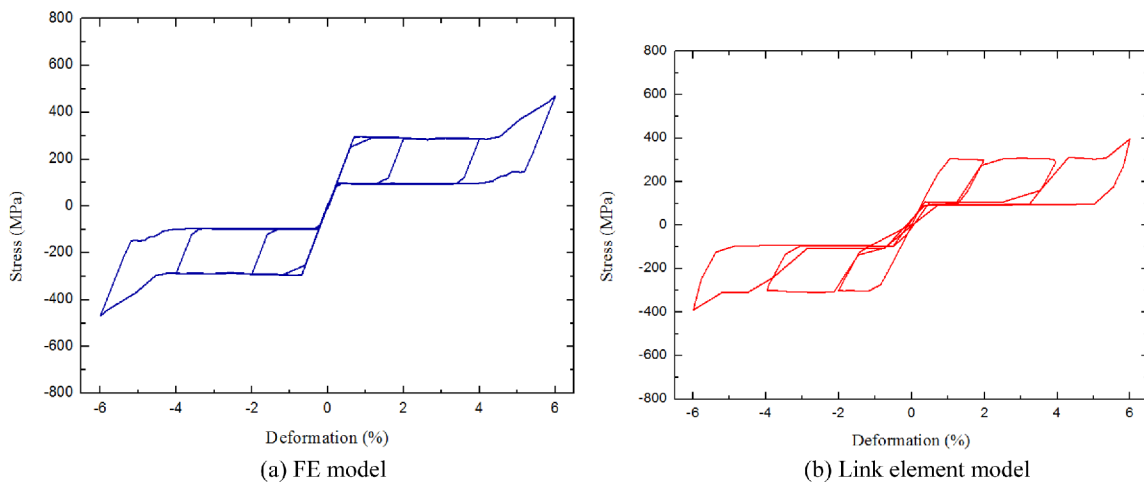


Figure 7. Axial stress vs. deformation curves of the SMA bar specimen 1 obtained from finite element and link element models.

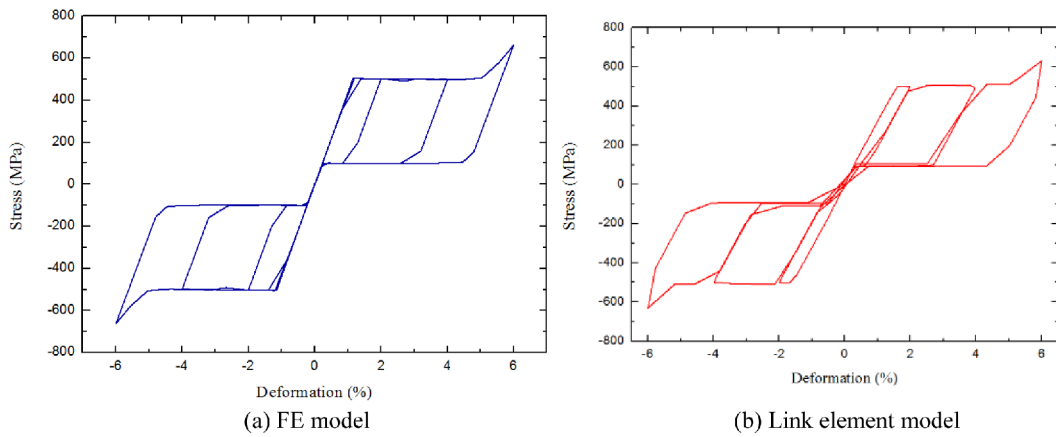


Figure 8. Axial stress vs. deformation curves of the SMA bar specimen 2 obtained from finite element and link element models.

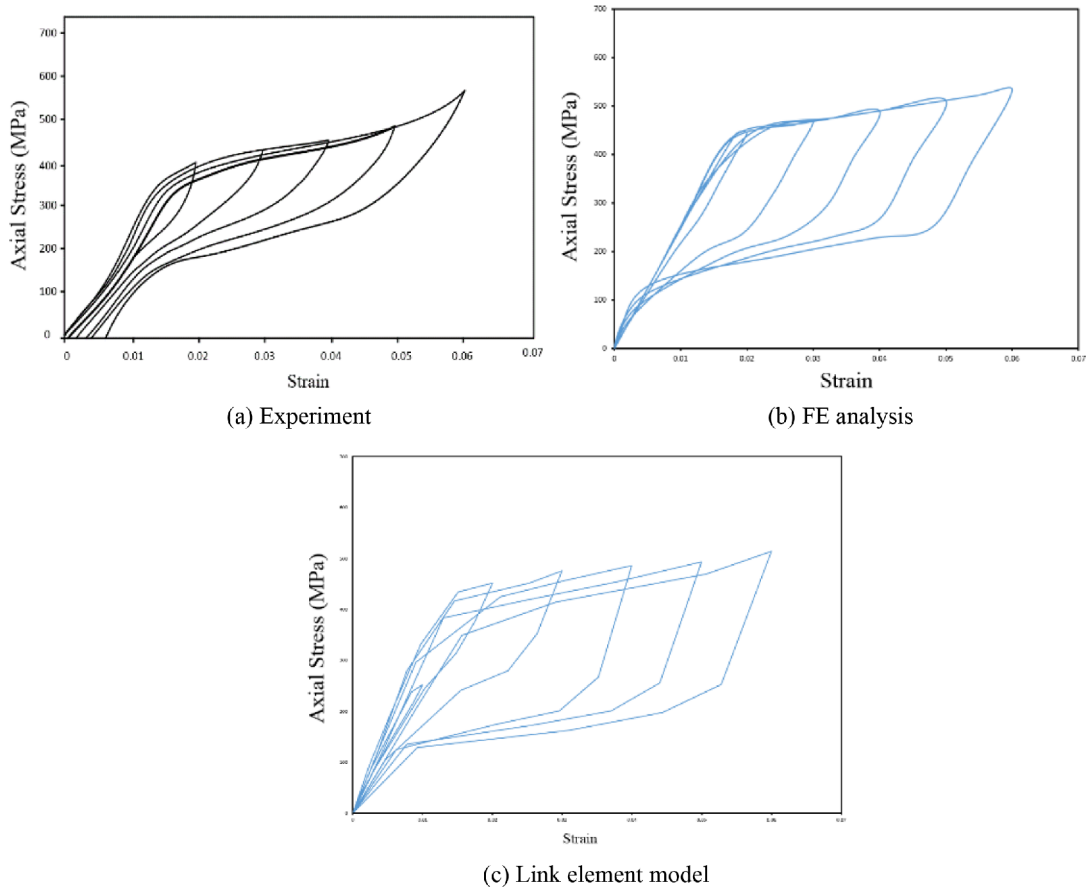


Figure 9. SMA bar stress-strain result obtained from (a) Experiment (b) FE analysis (c) Link element model.

the proposed and the FE models exhibit the symmetric hysteresis loops and superelastic effects of shape memory alloy. The proposed model for SMA is as accurate as the FE model and requires significantly less computational efforts.

Figure 9 compares the axial stress-strain curves of a SMA bar with diameter of 25 mm obtained by experiments of DesRoches *et al.* (2004), finite element analysis, and the multi-link model analysis. It can be observed that all

three results show similar skeleton curves under the same cyclic loading, and that the analysis results slightly overestimate the dissipated energy obtained from experiment.

5. Analysis of a Single Story Structure with a Slit Damper

The super elastic properties of shape memory alloy provide advantages over conventional steel damper in

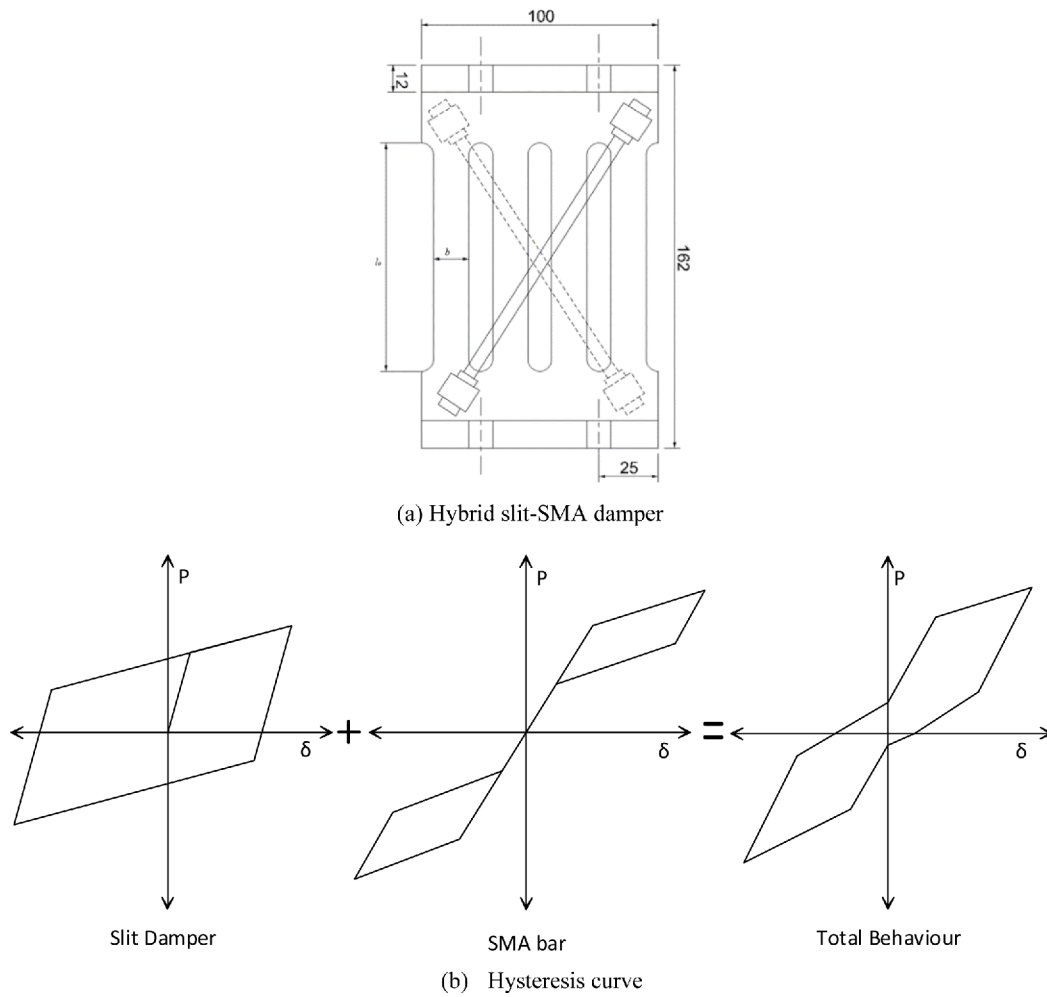


Figure 10. Shape and hysteresis curve of the slit damper with SMA bars.

terms of self-centering and fatigue-resisting capacities. However, due to high manufacturing cost, it is not economical to manufacture slit dampers solely with SMA material. To overcome the shortcomings of conventional steel slit damper and to achieve economy at the same time, in this study SMA bars are incorporated with steel slit damper. Using steel as base material and SMA as restrainer, re-centering capability can be provided to the slit damper to bring the structure back to its original position after an earthquake. This may significantly reduce the repair cost for structures whenever the structure is exposed to an earthquake.

Steel plate slit dampers are known to be an effective damping device for seismic retrofit of building structures (Kim and Jeong, 2016). The performance of slit dampers can be further enhanced by combining them with other damping devices (Kim and Shin, 2017; Lee et al., 2017). The yield load of the slit damper (P_y) can be defined under the plastic bending mechanism with the assumption of perfectly elasto-plastic material behavior as follows (Chan and Albermani, 2008):

$$M_p = \sigma_y \frac{tb^2}{4} \tag{1}$$

$$P_y = \frac{2nM_p}{l_0} = \sigma_y \frac{ntb^2}{2l_0} \tag{2}$$

where M_p indicates the full plastic moment when plastic hinges form at both ends of each strip with a rotation of θ_p , n indicates the number of strips, t and b are the thickness and width of the strip, respectively. The stiffness of the slit damper can be defined on the basis of an assumption that individual strips are fully constrained at their ends. It is determined as follows:

$$K = n \frac{12EI}{l_0} = n \frac{Etb^3}{l_0} \tag{3}$$

$$I = \frac{tb^3}{12} \tag{4}$$

where I is the moment of inertia of the prismatic strip.

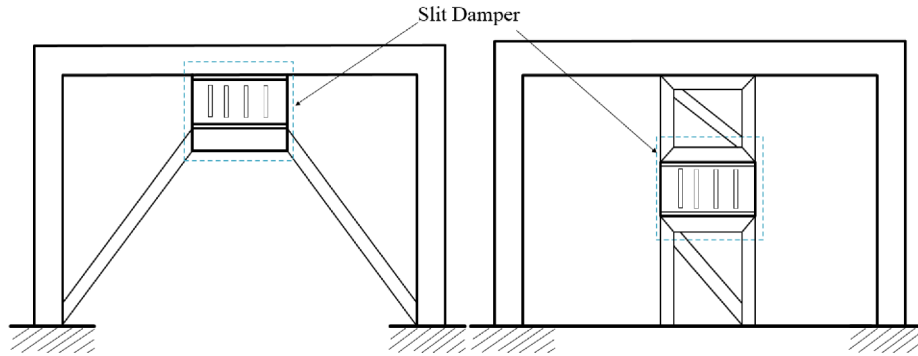


Figure 11. Installation of slit damper.

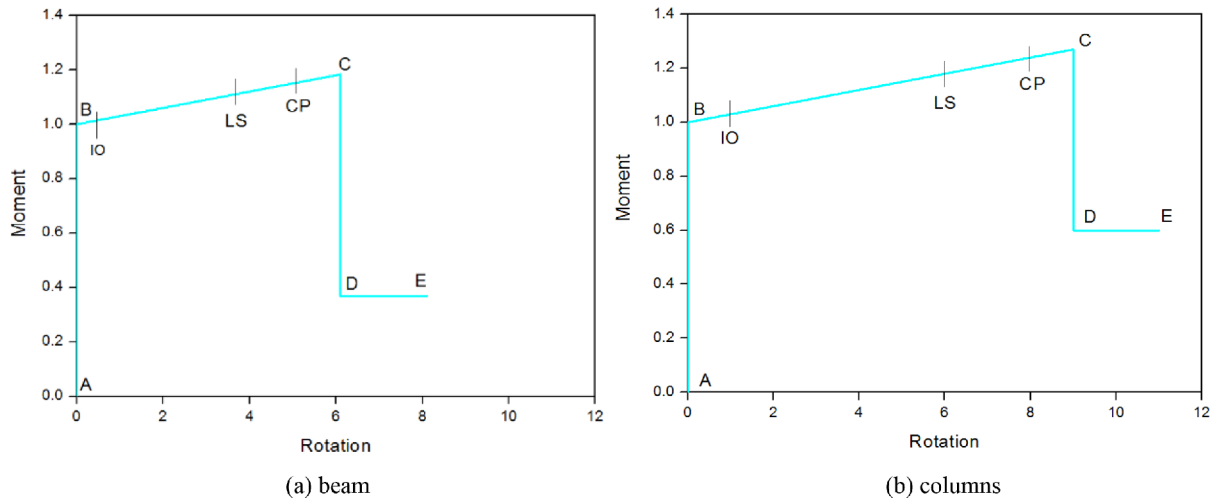


Figure 12. Nonlinear model for (a) beam and (b) columns.

The response mechanism of the slit-SMA hybrid damper includes the reverse phase transformation changing from martensite to austenite upon unloading which leads to self-centering behavior at the room temperature. The combined behavior of the hybrid damper can be obtained by superimposing superelastic behavior of SMA and the elasto-plastic behavior of slit damper. The total force of the hybrid damper can be determined by adding together component forces at the corresponding horizontal displacement (Δ) as shown in Fig. 10, as follows:

$$P = P_{SMA} + P_{Slit} \quad (5)$$

$$\Delta = \Delta_{SMA} + \Delta_{Slit} \quad (6)$$

The amount of permanent deformation in the hybrid damper is dependent on the re-centering force regulated by the size and material properties of the superelastic SMA bars.

In this section a single story steel moment frame with hybrid slit-SMA damper is analyzed for an earthquake ground motion. The geometric details of the slit damper used in this study are based on the test model of Chan and Albermani (2008). The dimensions and hysteresis curve of the hybrid damper are illustrated in Fig. 10, where the thickness steel plate is 8 mm and the height and the width

of the slit column are 149 and 9.7 mm, respectively. The hybrid damper is designed by installing SMA bars diagonally on both faces of a steel slit damper. The SMA bars are rigidly connected to the steel slit plate at both ends, and offer both stiffness and strength. It is assumed that the SMA bars do not resist compression due to buckling, and the two bars are installed in X shape so that at least one bar is subjected to tension during cyclic motion.

The damper is installed on the top of chevron (inverted-V) braces or between strong frames attached to the upper and lower beams as shown in Fig. 11. Typical steel slit dampers withstand shear forces carried from the beam members, and the slender strips deform in double curvature under bending and dissipate seismic energy by hysteretic damping. The beam and columns are made of W8×35 and W8×40 respectively and the following properties are assigned to the analysis model structures: floor weight 100 kN, story height $h=4.0$ m, width $L=6.0$ m, elastic modulus of steel = 210 GPa. Steel slit damper has the following properties: tensile yield stress = 316.5 N/mm², modulus of elasticity = 206.1 kN/mm², width to length ratio of a slit strip (b/l_0) = 0.155. Material properties of the SMA bars with 10 mm diameter are as follows: elastic modulus = 40 GPa, Poisson's ratio = 0.33, martensite start

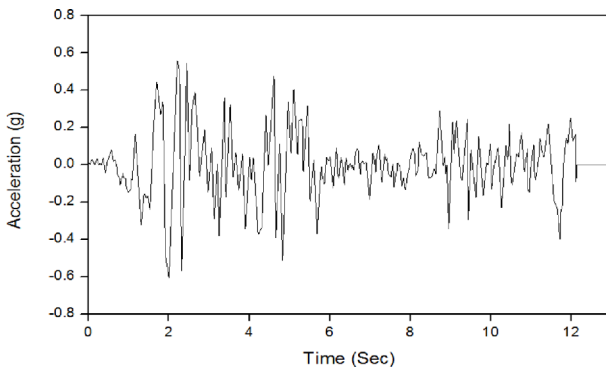


Figure 13. Ground acceleration of El Centro earthquake.

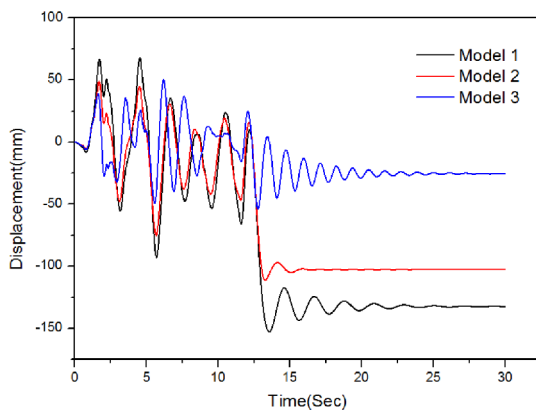
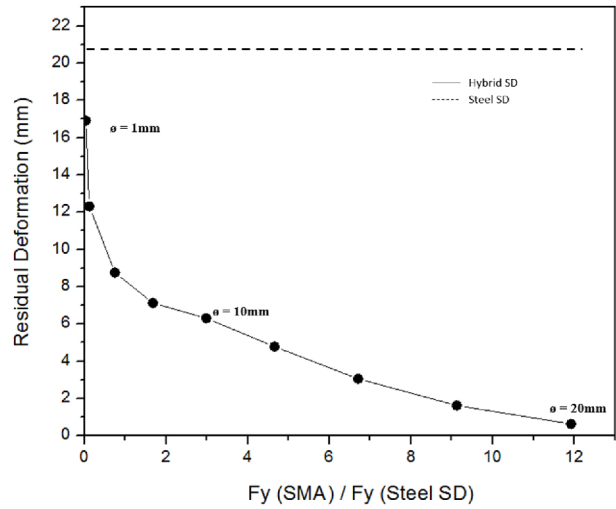


Figure 14. Displacement time history of the model structures.

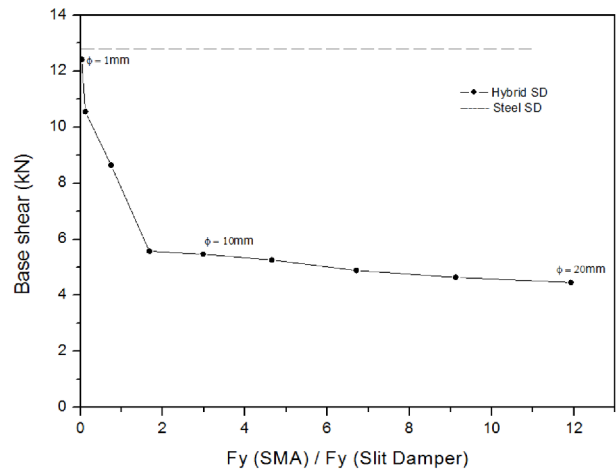
stress = 440 MPa, martensite finish stress = 540 MPa, austenite start stress = 250 MPa, austenite finish stress = 140 MPa, transformation strain = 0.042, phase transformation temperature = 22°C.

Nonlinear time history analyses are carried out using the El Centro earthquake record, scaled to the maximum peak acceleration of 0.6 g as shown in Fig. 13. The slit/SMA damper is modeled using the multi-link elements, and nonlinear dynamic analyses are carried out using SAP 2000. Figure 12 shows the nonlinear models for beam and columns provided in the FEMA 356 (2000). The locations of various deformation measures such as IO (immediate occupancy), LS (life safety), and CP (collapse prevention) are presented in the FEMA 356. Figure 13 shows the ground acceleration time history of the El Centro earthquake, and Fig. 14 shows the displacement time histories of the model structure subjected to the El Centro earthquake ground motion. It can be observed that the maximum roof displacement of structure (Model 1) is sufficiently reduced by the application of the slit damper (Model 2). The bare frame shows the largest residual deformation of 125 mm, while the residual displacement is reduced to 84 mm in the structure with steel slit damper (Model 3). However with SMA slit damper the structure is almost re-centered to its original position.

Parametric study is conducted to explore the effect of



(a) Residual displacement



(b) Base shear

Figure 15. Variation of the response for yield strength ratios of SMA bar and slit damper.

SMA bars on the re-centering of the system. For this purpose, SMA bars with different diameters are attached to the slit damper, which is installed in the single story model structure. Nine different diameters of SMA bars varying from 1 to 20 mm are installed on the slit damper one at a time, and nonlinear time history analysis are performed using the scaled El Centro earthquake. Figure 15 shows the variation of the residual displacement and base shear as a function of SMA size expressed as its yield strength with respect to the yield strength of the slit damper. The horizontal dotted line in Fig. 15(a) represents the residual displacement of the system with the steel slit damper without SMA bar. It can be observed that as the size of the SMA bar increases the residual displacement and the base shear keeps decreasing. The rate of reduction of residual displacement decreases as the diameter of the SMA bar exceeds 7.5 mm, and that of the base shear decreases as the diameter of the SMA bar exceeds 10.5

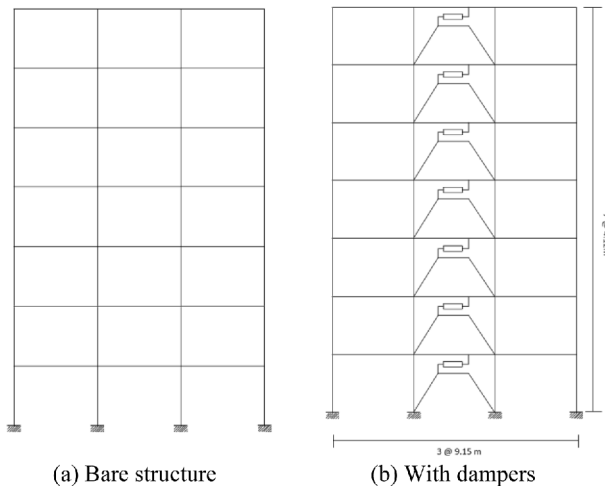


Figure 16. Seven story frame analysis mode.

mm. When the SMA bar with 20 mm diameter is installed, the residual displacement decreases less than 1 mm.

5. Seismic Response of Structure with Hybrid Dampers

The seven story structures shown in Fig. 16 are used to investigate the seismic response of structure with steel slit dampers and hybrid dampers with a 10 mm diameter SMA bar attached to each side of the slit plate damper. The analysis model frames are designed according to ASCE 7-13 (2013) using the dead load of 4.12 kPa and live load of 2.39 kPa throughout the stories, and the wind load with the basic wind speed of 30 m/s at the height of 10 m from the ground level. The yield stress of the structural steel is 330 MPa for beams and columns. The fundamental natural periods of the bare frame structure is 2.1 sec. computed from eigenvalue analysis. For the dynamic analysis, story masses are placed in the story levels considering rigid diaphragm action. For the modeling of nonlinear beam and columns in steel, the flexural hinges provided in the FEMA 356 are used.

Nonlinear time-history analysis is carried out using the

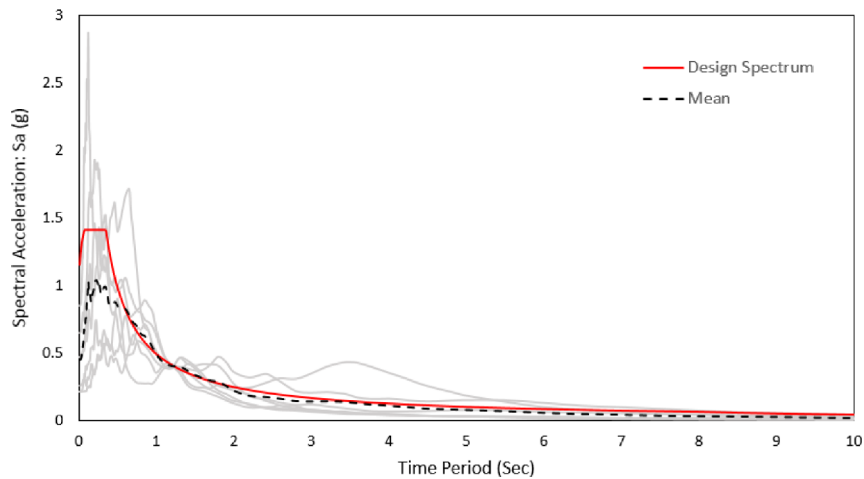


Figure 17. Response spectra for the seven ground motions scaled to fit the design spectrum for LA area.

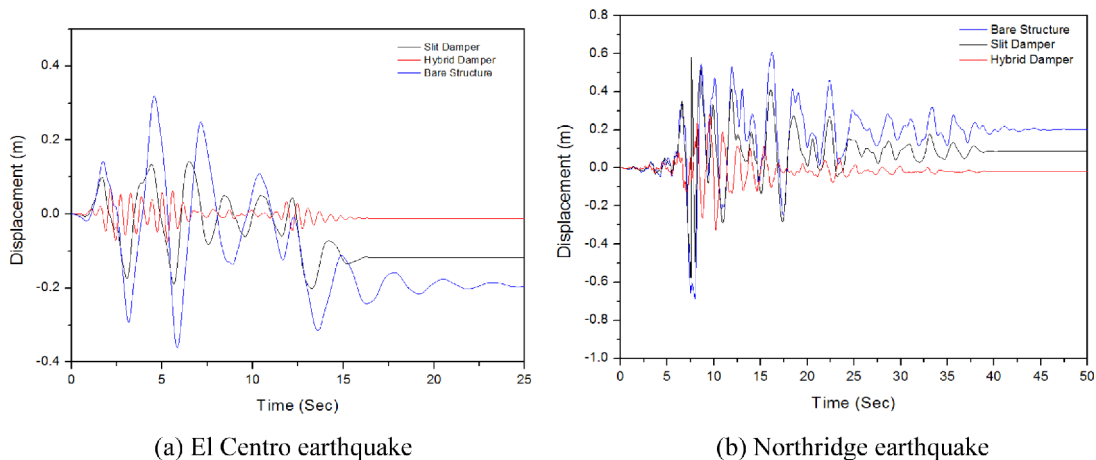
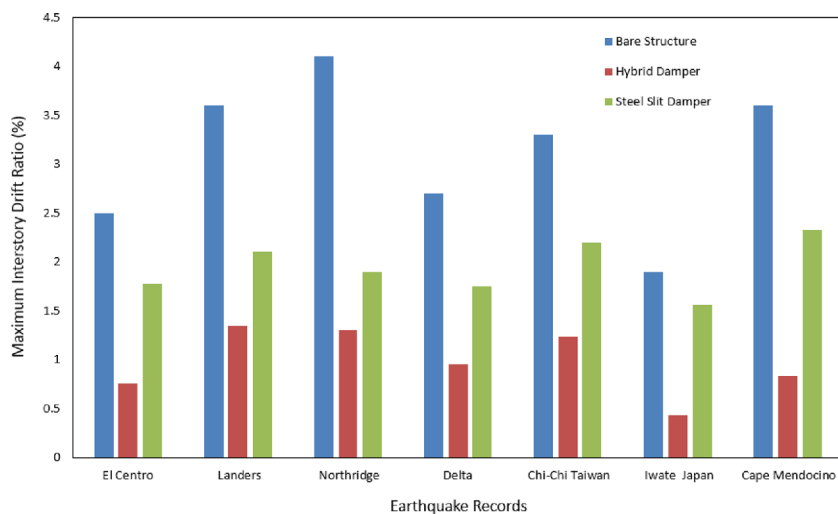
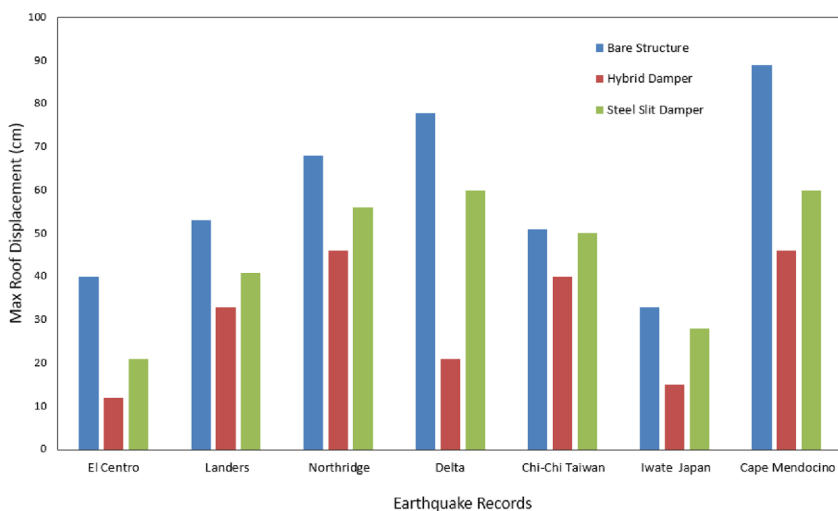


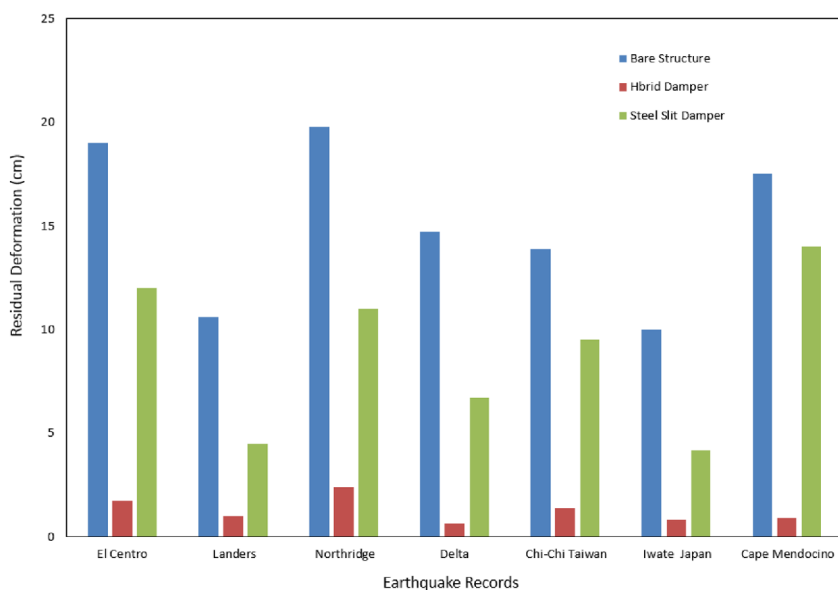
Figure 18. Time history of roof displacement of bare frame, hybrid re-centering frame and steel slit damper frame.



(a) Maximum inter-story drift ratio



(b) Maximum roof displacements



(c) Residual deformation

Figure 19. Maximum responses of the analysis models for the seven ground motion records.

seven earthquake records scaled to the design spectrum to validate the efficiency of the shape memory alloy bars attached to a conventional slit damper in reducing the maximum and residual drifts of existing structure. The response spectra of the ground motions scaled to fit the design spectrum for LA area are shown in Fig. 17. The spectral acceleration parameters S_{DS} and S_{D1} are 1.40 and 0.48, respectively, with site class D.

The roof displacement time histories of the model structures for El Centro ground motion and Northridge ground motions are presented in Fig. 18. The peak roof displacements of the bare frame are approximately 38 cm and 67 for the El Centro and the Northridge earthquakes, respectively. On the other hand, that of the structure equipped with hybrid slit-SMA dampers is reduced to 12 and 34 cm, respectively. It also can be observed that, after a certain time is elapsed the center of oscillation is shifted due to the plastic deformation in the bare structure and the structure with slit dampers. The residual deformations at the end of the El Centro and the Northridge ground excitations are reduced from 19 and 21 cm to approximately 1.7 and 2.4 cm with the hybrid dampers, respectively. This shows the potential of SMA to bring the structure back to its original position while providing supplemental damping and stiffness for reducing the maximum displacement as well. In the case of Northridge earthquake excitation, residual deformation reduces to 2.4 cm in the frame equipped with hybrid slit damper, and the maximum displacement is reduced to 30% of that of the model structure with slit dampers.

Figure 19 shows the maximum inter-story drifts and the maximum and the residual roof displacements of the analysis models for the seven ground motion records. It can be observed in Fig. 19(a), 19(b) and 19(c) that there are sufficient reductions in the residual deformation, maximum inter-story drift and reduction in maximum roof displacements of the model structure installed with hybrid dampers when compared with those of the structure with steel slit dampers or the bare structure. There is an average reduction of 68 and 48% in the maximum inter story drift and the maximum roof displacement, respectively, as compare to those of the bare structure. Compared with the maximum responses of the structure with steel slit dampers, there are approximately 49 and 35% reduction in the maximum inter-story drift and the maximum roof displacement, respectively. The most significant reduction in the responses of the structure with hybrid dampers can be found in the residual roof displacement of the structure equipped with hybrid dampers as can be observed in Fig. 19(c) which is more than 80%. This result highlights the advantage of SMA bars in conjunction with steel slit damper.

6. Conclusions

In this paper a hybrid energy dissipation device was

developed by combining a SMA bar and a steel slit plate. An analysis modeling of a SMA bar with super elastic capability was developed using various link elements such as hook, gap, bilinear elastic and plastic elements, etc., and the accuracy of the analysis model was verified by comparing with finite element analysis results. The seismic performance of the hybrid slit damper was verified by incorporating them in seven story steel structure with slit and hybrid slit-SMA dampers.

According to the analysis results the link element modeling of the SMA bar turned out to produce the superelastic behavior of the bar quite similar to that produced by sophisticated finite element method. The nonlinear dynamic analysis results of the model structure subjected to seven earthquake ground motions showed that the addition of SMA bars in slit damper results in significant reduction in both the maximum and residual displacements. In the model structure with conventional steel slit dampers the average maximum inter story drift and the maximum roof displacement of the model structure were reduced by, respectively, 35 and 22% in comparison with those of the bare frame. The addition of a $\Phi=10$ mm SMA bar in a slit damper resulted in 68 and 48% reduction in the maximum inter story and the roof displacements of the model structure. In addition more than 80% reduction was observed in the residual deformation at the roof story compared to those of the structure installed with typical steel slit dampers. These results indicate that the hybrid slit-shape memory alloy (SMA) energy dissipation device has a potential to be used as an effective seismic design and retrofit tool for structures. It should be pointed out that the analysis results of the link element model presented in this study were verified only by more rigorous finite element analysis; however for further validation of the proposed analysis model the analysis results needs to be further verified by proper experimental data.

Acknowledgment

This research was supported by Basic Science Research Program through the National Research Foundation of Korea (NRF) funded by the Ministry of Education (NRF-2017R1D1A1B03032809).

References

- ANSYS (2012), Mechanical APDL (Release 14.0). ANSYS Inc. Canonsburg, US
- Andrawes B, DesRoches R (2005). "Unseating prevention for multiple frame bridges using superelastic devices." *Smart materials and structures*, 14(3), S60.
- Cardone D, Dolce M, Ponzo FC (2004). "Experimental behaviour of R/C frames retrofitted with dissipating and re-centring braces." *Journal of Earthquake Engineering*, 8(03), pp. 361-396.
- Chan RW, Albermani F (2008). "Experimental study of steel slit damper for passive energy dissipation." *Engineering*

- Structures*, 30(4), pp. 1058-1066.
- Clark PW, Aiken I, Kelly JM, Krumme R (1995). Experimental and analytical studies of shape-memory alloy dampers for structural control. *Smart Structures & Materials' 95*, International Society for Optics and Photonics.
- DesRoches, R., McCormick, J, Delemont, M (2004). "Cyclic properties of superelastic shape memory alloy wires and bars." *Journal of Structural Engineering*, 130(1), pp. 38-46.
- Dolce M, Cardone D, Marnetto R (2000). "Implementation and testing of passive control devices based on shape memory alloys." *Earthquake Engineering & Structural Dynamics*, 29(7), pp. 945-968.
- FEMA 356, Prestandard and Commentary for the Seismic Rehabilitation of buildings, Federal Emergency Management Agency, Washington, D.C., 2000
- Fremont, M. (1996). Shape memory alloy, Springer.
- Han YL, Li QS, Li AQ, Leung AYT (2003). "Structural vibration control by shape memory alloy damper." *Earthquake Engineering & Structural Dynamics*, 32(3), pp. 483-494.
- Ingalkar, Rameshwar. S. (2014). Rehabilitation of Buildings and Bridges by Using Shape Memory Alloys (SMA). *International Journal of Civil Engineering Research*, 5(2), pp. 163-168.
- Jalaeefar A, Asgarian B (2014). A simple hybrid damping device with energy-dissipating and re-centering characteristics for special structures. *The Structural Design of Tall and Special Buildings*, 23(7), pp. 483-499.
- Kim J, Jeong J (2016). "Seismic retrofit of asymmetric structures using steel plate slit dampers", *Journal of Constructional Steel Research*, 120, pp. 232-244
- Kim J, Shin H (2017). "Seismic loss assessment of a structure retrofitted with slit-friction hybrid dampers", *Engineering Structures*, 130, pp. 336-350
- Lee J, Kang H, Kim J (2017). "Seismic performance of steel plate slit-friction hybrid dampers", *Journal of Constructional Steel Research*, 136, pp. 128-139.
- Ma H, Cho C (2008). "Feasibility study on a superelastic SMA damper with re-centring capability." *Materials Science and Engineering: A* 473(1), pp. 290-296.
- McCormick J, Aburano H, Ikenaga M (2008). Permissible residual deformation levels for building structures considering both safety and human elements. *Proceedings of the 14th world conference on earthquake engineering*.
- McCormick J, DesRoches R, Fugazza D (2007). "Seismic assessment of concentrically braced steel frames with shape memory alloy braces." *Journal of Structural Engineering*, 133(6), pp. 862-870.
- Miller DJ, Fahnestock LA, Eatherton MR (2012). Development and experimental validation of a nickel-titanium shape memory alloy self-centering buckling-restrained brace. *Engineering Structures*, 40, pp. 288-298.
- Ocel J, DesRoches R, Leon RT, Hess WG (2004). "Steel beam-column connections using shape memory alloys." *Journal of Structural Engineering*, 130(5), pp. 732-740.
- Ozbulu, OE, Hurlbaeus S (2012). Application of a SMA-based hybrid control device to 20-story nonlinear benchmark building. *Earthquake Engineering & Structural Dynamics*, 41(13), pp. 1831-1843.
- Saadat S, Salichs J, Noori M, Hou Z (2002). "An overview of vibration and seismic applications of NiTi shape memory alloy." *Smart materials and structures*, 11(2), pp. 218.
- SAP (2010). Analysis Reference Manual. *Computer and Structures*, Berkeley.
- Song G, Ma N, Li HN (2006). "Applications of shape memory alloys in civil structures." *Engineering Structures*, 28(9), pp. 1266-1274.
- Tamai, H. and Y. Kitagawa (2002). "Pseudoelastic behavior of shape memory alloy wire and its application to seismic resistance member for building." *Computational materials science*, 25(1), pp. 218-227.
- Tanaka T, Chung SW, Chaing LF, Makii K (2004). "Post-characteristics of formed Zn-22 mass% Al alloy to seismic damper for general residence." *Materials transactions*, 45(8), pp. 2542-2546.
- Torra V, Isalgue A, Auguet C, Carreras G, Lovey F, Terriault P (2013). Damping in civil engineering using SMA Part 2-particular properties of NiTi for damping of stayed cables in bridges. *Canadian Metallurgical Quarterly*, 52(1), pp. 81-89.
- Wilde K, Gardoni P, Fujino Y (1997). Seismic response of base-isolated structures with shape memory alloy damping devices. *Smart Structures and Materials' 97*, International Society for Optics and Photonics.
- Wierschem N, Andrawes B (2010). Superelastic SMA-FRP composite reinforcement for concrete structures. *Smart materials and structures*, 19(2), 025011.
- Yan, X. and J. Nie (2003). "Study of a new application form of shape memory alloy superelasticity." *Smart materials and structures*, 12(6), N14.